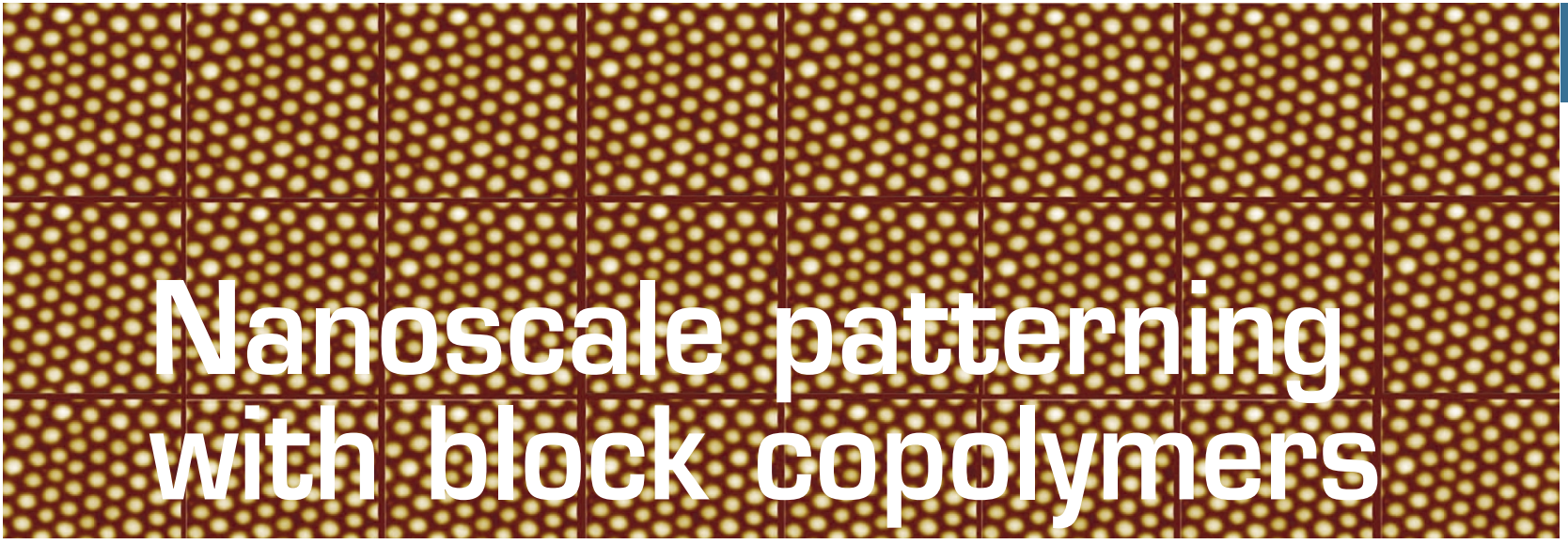

Nanoscale patterning with block copolymers

The self-assembly processes of block copolymers offer interesting strategies to create patterns on nanometer length scales. The polymeric constituents, substrate surface properties, and experimental conditions all offer parameters that allow the control and optimization of pattern formation for specific applications. We review how such patterns can be obtained and discuss some potential applications using these patterns as (polymeric) nanostructures or templates, e.g. for nanoparticle assembly. The method offers interesting possibilities in combination with existing high-resolution lithography methods, and could become of particular interest in microtechnology and biosensing.

Sivashankar Krishnamoorthy, Christian Hinderling, and Harry Heinzelmann*
Centre Suisse d'Electronique et de Microtechnique, CSEM, Jaquet Droz 1, 2002 Neuchâtel Switzerland
**E-mail: harry.heinzelmann@csem.ch*

The continued development of lithography technologies allows patterns to be produced with feature sizes well below 100 nm. However, the increasing cost and complexity of lithography puts serious doubts on the sustainability of the International Technology Roadmap for Semiconductors. Other ways of creating structures in the ~10-100 nm range may represent alternatives if they offer advantages in reduced production cost, smaller feature sizes, or more flexibility regarding the material or function of the nanometric structures[1-3]. Systems that show ordering and pattern formation through self-assembly processes may offer some of these advantages, although in general they suffer from the limitation that only periodic or quasiperiodic structures can be obtained. Among these self-assembly approaches, nanopatterning using block copolymers has attracted much attention[4-6].

Block copolymers are a special class of polymer with two or more polymer chains (or blocks) chemically bound to each other. The simplest in the class are diblock copolymers where two chains are bound to each other through a covalent linkage. Since different polymers do not mix well for entropic reasons, especially if their molecular weight is sufficiently high, they have a strong tendency to form separate phases. In a block copolymer, this phase separation has to occur intermolecularly; the two blocks can only separate to a distance compatible with the size of the chains. This constraint leads block copolymers to separate into periodic microphases, i.e. into domains that are each rich in one of the constituent blocks. The size of the domains is on the order of the size of the macromolecules, i.e. ~10-100 nm. The properties of the constituent polymers, the number of monomeric units in each block, along with the relative proportion of the polymers within the block copolymer determine the resulting equilibrium morphologies. The morphologies that represent different phases are dictated by the Flory-Huggins interaction parameter χ and the volume fraction of the blocks ϕ. If the volume fractions of the

ISSN:1369 7021

blocks are close to equal, a layered morphology is often observed. When moving toward less equal block ratios, the observed morphologies go through a bicontinuous gyroid structure, hexagonally packed cylinders, and finally body-centered-cubic-packed spherical domains. On surfaces, this microphase separation results in nanoscale structures (domains) with sub-100 nm length scales. In addition, the surface contributes to the type of nanopatterns obtained.

The salient features of the nanostructures, such as their material composition, morphology, dimensions, spacing, and order are of primary significance for the chemical, mechanical, optical, and electromagnetic properties they exhibit. The design of block copolymers with controlled properties allows their application as surfaces with tunable wettabilities, increased cell adhesion, large surface-to-volume ratios for chemo- and biosensing, and etch resistant patterns for further processing.

We describe approaches based on block copolymers for producing functional nanoscale structures on surfaces. Emphasis is put on the tunability and responsiveness of diblock copolymer films on surfaces where relevant for their use in nanofabrication. The use of block copolymer patterns to form nanoparticle arrays, and the transfer of copolymer patterns to form corresponding structures in various materials, are presented.

Nanopatterns from block copolymers

Block copolymer thin films (typically <100 nm thick) coated on a flat substrate using spin-coating, dip-coating, or drop-coating exhibit a wide variety of patterns. Block copolymer nanopatterns on surfaces can exhibit significant deviations from their bulk morphologies. Transmission electron microscopy (TEM), scanning electron microscopy (SEM), and atomic force microscopy (AFM) have revealed that the characteristics of the patterns are significantly influenced by parameters such as the film thickness, solvent selectivity, and substrate interactions in combination with the molecular characteristics of the copolymer.

Influence of the substrate and polymer film thickness

When block copolymer solutions are made using a nonselective solvent (a solvent that shows no selectivity for any of the polymer blocks), the polymer is molecularly dissolved and a thin film of the polymer can exhibit characteristic morphologies even as-coated. The polymer films can be annealed above the glass transition temperature T_g of the constituent polymers in order to enhance the ordering of the domains.

Thin films of block copolymers are constrained by the presence of the polymer-air and polymer-substrate interfaces as boundaries, in addition to the film thickness being either an integer or a noninteger multiple of the bulk domain periodicity L_0. Hence, pattern formation is dictated by the preference of the polymeric blocks for one or both of the interfaces, as well as the total film thickness. The properties of the substrate-polymer interface can be modified by tuning the surface chemistry to achieve perpendicular orientation of cylinder- or lamella-forming diblock copolymer systems. This has been achieved by neutralizing the substrate surface using random copolymer brushes[7,8] and self-assembled monolayers (SAMs)[9-11].

The influence of the film thickness t in relation to L_0 has also been investigated. While for films of thickness $t > L_0$, terrace defects of height L_0 form on the surface[12], films of thickness $t < L_0$ are subject to frustration induced by various competing forces[13-16]. These competing forces include strong surface interactions, slow kinetics, and a driving force toward achieving the bulk periodicity. Polystyrene-*block*-poly(2-vinylpyridine) (PS-*b*-P2VP) thin films with $t < L_0$ have been shown to form characteristic surface-induced nanopatterns (SINPAT) on mica, driven by strong P2VP-mica interactions[17]. This dependence of the copolymer morphology on film thickness has been exploited through topographic patterning to achieve desired patterns[18]. Deviations from bulk morphology driven by the constraints imposed by two-dimensional confinement in thin films result in various morphologies, such as perforated lamellae and lamellae (Fig. 1)[19,20].

The influence of the substrate has been exploited to achieve large-scale domain alignment and ordering. Rockford *et al.*[21] and Yang *et al.*[22] have used chemically heterogeneous surfaces to control macromolecular ordering. Segalman and colleagues[23] have introduced the use of surface relief grating structures to enhance positional order of PS-P2VP copolymer thin films over large areas. Their graphoepitaxy approach can be carried out with substrate topographies <5 μm in depth, which is amenable to photolithographic processing. Kim *et al.*[24] have used extreme ultraviolet (EUV) lithography to pattern SAM-coated substrates. The ordering of polystyrene-*block*-poly(methylmethacrylate) (PS-*b*-PMMA) lamellae could then be

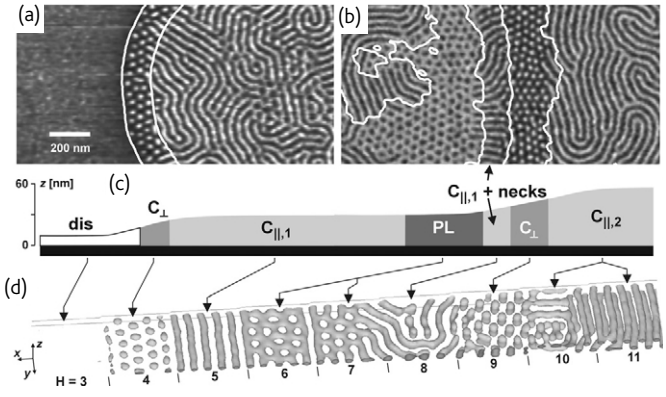

Fig. 1 (a, b) Tapping mode AFM phase image of a styrene-butadiene-styrene (SBS) triblock copolymer after solvent annealing. The film forms domains with different thicknesses in which different morphologies and orientations are observed. White contour lines calculated from the corresponding height images are superimposed. (c) Schematic height profile of the phase images. (d) Simulated structure of an $A_3B_{12}A_3$ block copolymer with increasing film thickness. $C_\perp$, $C_{//}$, cylindrical morphology arranged perpendicular and parallel to the substrate, respectively; PL, perforated lamellae. (Adapted from[18] and reprinted with permission. © 2002 American Physical Society.)

influenced over areas greater than 8 x 5 μm^2. The alignment of the lamellae was shown to be perfect when the periodicity of the SAM pattern matched the natural domain spacing of the diblock copolymer. This approach, although elegant from a scientific point of view, poses tough demands on processing costs and is not high throughput. Xiao *et al.*[25] have demonstrated use of nanoporous PS templates derived from a topographically induced perpendicularly aligned PS-PMMA diblock copolymer as a mask for creating Ni nanodots arrays.

Nanopattern confinement through top-down approaches

Confinement of nanopatterns within addressable micro- or submicron-sized patterns is important to derive substantial benefits from the nanostructure properties. In order to make the nanopatterns addressable, extend patterning capabilities to nonperiodic structures, and improve ordering in periodic patterning, different combinations of self-assembly have been investigated. These include templated self-assembly and graphoepitaxy, as well as mix-and-match strategies.

The graphoepitaxy approach for achieving confinement-induced ordering has been employed by Cheng *et al.*[26] to serve as a means for confining nanostructures to areas defined by photolithography. This technique is not very convenient for defining nanopatterns within nonperiodic regions. Electron-beam (e-beam) lithography has been used by Glass *et al.*[27,28] to pattern PS-P2VP micelles into a variety of periodic and nonperiodic areas. In this work, the immobilization of micelles to selected regions on conducting as well as nonconducting surfaces was carried out by crosslinking them using the e-beam (Fig. 2). Furthermore, prestructures generated on a surface using e-beam lithography could even help confine single micelles upon dipping and withdrawal from a micellar solution. This provides an elegant means of separating single or groups of nanostructures into patterns on a surface. However, the process is less attractive given its expense and low throughput. Top-down methods of modifying copolymer patterns can be achieved using localized modification of copolymer micellar thin films using deposition of selective solvents by printing or nanodispensing[29].

At present, however, general methods for efficient top-down patterning of nanopatterns into periodic and aperiodic areas on a surface that are high throughput and have wafer-level process compatibility are still lacking.

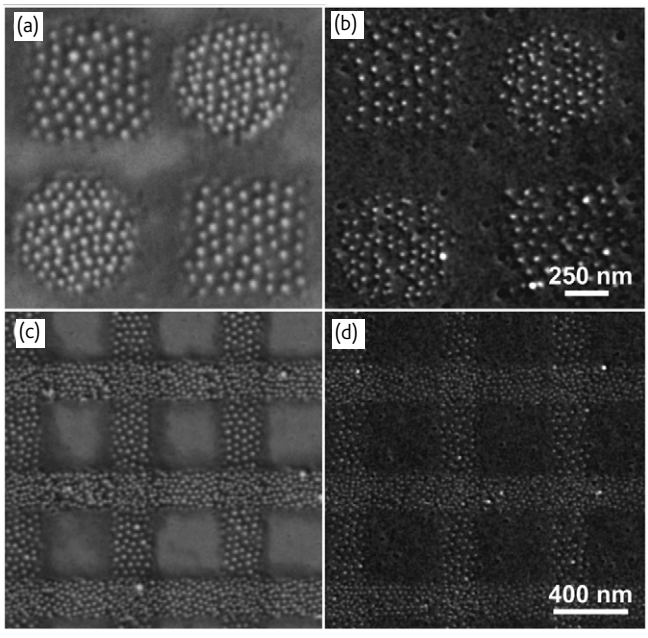

Fig. 2 SEM images before (a, c) and after (b, d) plasma treatment. Diblock copolymer micelles from PS(500)-b-P[2VP(HAuCl$_4$)$_{0.5}$](270) and PS(990)-b-P[2VP(HAuCl$_4$)$_{0.5}$](385) were deposited consecutively on a carbon-coated glass cover slip, followed by e-beam writing and dimethylformamide lift-off processing. Finally, samples were exposed to a hydrogen gas plasma. This resulted in deposition of ~5-6 nm diameter Au particles in two differently spaced patterns (57 nm or 73 nm). (Adapted and reprinted with permission from[28]. © 2004 Institute of Physics.)

Copolymer micelle formation

A further very general way of generating surface nanostructures from block copolymers lies in the controlled deposition of aggregates preformed in solution, i.e. block copolymer micelles, onto substrates. This approach allows access to additional handles to influence and tune the obtained patterns by changing easily accessible experimental variables like solvent quality or deposition conditions.

Block copolymer micelles form when the polymers are dissolved in a selective solvent, i.e. a solvent in which only one of the polymer blocks dissolves well. This drives aggregation of the copolymer molecules to form micelles with an insoluble core and a soluble corona (shell). Micellar structures are of great utility as templates for creating nanoparticle arrays[30] and in lithographic applications[31]. Micelles are kinetically frozen if the core-forming block is in the glassy state (i.e. the temperature is below T_g and the polymer is not swollen to an appreciable extent by the solvent) and the form is not retained upon annealing. The selectivity of the solvent used significantly influences the morphology and dimension of the micelles obtained. Fu *et al.*[32] have investigated the self-assembly of a poly-L-lactic acid-*block*-polystyrene (PLLA-*b*-PS) diblock copolymer in neutral, slightly selective, and highly selective solvents. Choucair *et al.*[33] have reviewed a variety of means of tuning micelle morphologies by controlling the environment of micelle formation.

Spherical micelles, which are the most common shape, are useful in creating ordered hexagonal arrays on surface, even in as-coated form[34]. This offers several advantages, since the array inherently offers a nanoscale periodic contrast in both topography and chemistry[35]. In contrast, thin films coated from a nonselective solvent require appropriate post-processing steps to be able to achieve the same objective. The use of micelles as templates is covered more in detail in following sections.

Tunability of nanopatterns

Many approaches have been developed to tune the size, shape, and spacing of block copolymer domains and the nanostructures derived from them. The primary means of realizing this have been through (1) changing the relative lengths of the blocks and (2) the total block-copolymer molecular weight.

Xu *et al.*[36] have obtained porous films with hexagonal arrays of pores with varying diameters from 14-50 nm and periodicities from 24-89 nm by changing the molecular weight of cylinder-forming PS-PMMA diblock copolymers. The results show the dependence of the lattice periodicity L_0 on the degree of polymerization N is $L_0 \sim N^{2/3}$, which conforms to predictions for block copolymers in the strong segregation limit. Guarini *et al.*[37] have obtained nanoporous templates derived from PS-PMMA with pore diameters of 20 nm and 30 nm and lattice periodicities of 42 nm and 62 nm by using copolymers with molecular weights of 67 kDa and 132 kDa, respectively. The interpore separation distance shows a power law dependence on the copolymer molecular weight, as shown by earlier theoretical and experimental work. This allows for systematic tuning of template dimensions by using block copolymers with different molecular weights. This is of great importance given the applications these templates have been put to, such as creating Co nanowire arrays[38,39], nanoparticle arrays[40,41], and nanostructure replication on hard and soft surfaces.

The addition of a homopolymer provides an attractive means of tuning both the morphology and the domain size, as well as the spacing attainable with a neat block copolymer thin film. Such blends of homopolymers, homopolymers with block copolymers, and blends of block copolymers form interesting patterns. Whether the homopolymer addition causes a change in morphology or only changes in the spacing of the domains depends on the molecular weight of the homopolymer added and its volume fraction in the blend[42]. The dependence of the homopolymer dissolution and distribution within the block copolymer microdomains upon homopolymer molecular weight and volume fraction has been examined in detail[43-46].

The dimensions and spacing of micellar nanostructures obtained by dissolving amphiphilic diblock copolymers in selective solvents can be tuned systematically. We have recently demonstrated variation of the characteristic dimensions of two-dimensional PS-P2VP micelle arrays on a Si surface by varying solvents, conditions of deposition, and by using solvent mixtures of varying compositions (Fig. 3). The advantage of this approach lies in the fact that the tunability is achieved with a copolymer of same molecular weight. This is interesting given that the micelles can be used as a template for creating nanoparticles or for transferring structures into a surface. Thus, any tunability achieved in micelle dimension and array periodicity will be of benefit to achieving particle arrays or pillar arrays with various characteristic dimensions.

Responsive nanopatterns derived from surface reconfiguration of block copolymers

The selective swelling or modification of one of the copolymer microdomains can cause *in situ* morphological changes that result in interesting chemically and topographically nanopatterned surfaces.

La *et al.*[47] have recently demonstrated a cylinder to sphere transition in polystyrene-*block*-poly-*t*-butylacrylate (PS-*b*-PtBuA) diblock copolymer films. They exploited the thermal-deprotection-induced volume fraction change of the PtBuA blocks. Starting from large-area cylinders of PS-PtBuA aligned parallel to the surface, they created highly ordered arrays of spherical PS-PAA domains.

Sidorenko *et al.*[48] have demonstrated an elegant approach to derive reactive membranes and nanotemplates based on supramolecular assembly of a polystyrene-poly-4-vinylpyridine (PS-P4VP) diblock copolymer with 2-(4'-hydroxybenzeneazo) benzoic acid (HABA). This supramolecular assembly on a surface is responsive to solvent vapors, driving the P4VP cylindrical domains to orient parallel or perpendicular to the surface. Furthermore, nanopores of 8 nm diameter and 24 nm periodicity, decorated with P4VP functionality, were used as templates for creating high-density metallic nanodot arrays using electrodeposition.

Surface reconfiguration of block copolymer films can be achieved by exploiting preferential interaction of solvents with one of the blocks. Xu *et al.*[49,50] have shown a solvent-induced reconfiguration of PS-PMMA diblock thin films that results in the formation of a nanoporous template. The preferential interaction of acetic acid with the PMMA block is responsible for forming the nanopores. The original structure is regained upon annealing above the T_g of the copolymer.

Sohn *et al.*[51] have reported switchable nanopatterns formed by core-corona inversion of free-standing PS-P4VP reverse micelle monolayer films. The *in situ* core-corona inversion occurs upon exposure to methanol, which can then be reversed by toluene. The switchable nanopatterns can be transferred to any substrate.

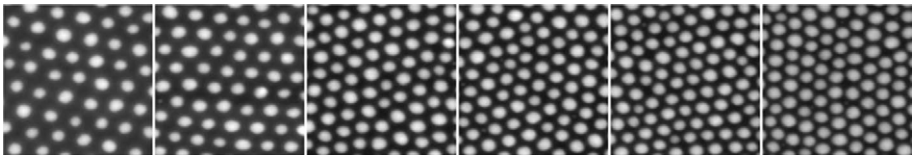

Fig. 3 Tapping-mode AFM micrographs of arrays of PS-b-P2VP reverse micelles spin-coated onto Si substrates. The spacing of the features can be tuned systematically over a wide range by using solutions of micelles of different concentrations. The z-scale is 50 nm with a 1 μm x 1 μm scan size. (Adapted and reprinted with permission from[35]. © 2006 Wiley-VCH.)

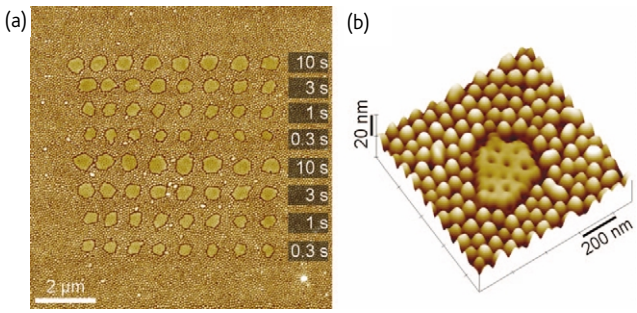

Fig. 4 (a) Monolayers of PS-P2VP micelles that have been locally modified by depositing attoliter quantities of glycerol using a hollow AFM tip as dispenser. The size of the spots can be controlled by the contact time of the AFM tip (shown for each line) with the surface. (b) Detail of one of the smaller spots. (Adapted and reprinted with permission from[29]. © 2006 Elsevier.)

We have used a similar PS-P2VP micellular thin film transformation to create Si pillars and holes[31]. This transformation is independent of the substrate used, making the approach more versatile and adaptable for structuring other hard surfaces. Meister *et al.*[29] have shown highly localized modification of PS-P2VP micelle monolayers by deposition of glycerol using nanoscale dispensing (NADIS) via a hollow AFM tip (Fig 4). Elbs *et al.*[52] have used solvent-vapor-induced characteristic morphological changes to study different phases at the surface.

Surface reconfiguration of PS-PMMA and PS-P2VP films also results in a change in surface energy depending on the block that is exposed to the surface[50]. This is similar to changes seen in surface energy with surface-grafted amphiphilic block copolymer films, but it is simpler as a grafting step is not necessary[53]. Grafting also demands appropriate surface chemistry and pretreatment conditions to begin with, making the approach less universal.

Block copolymer nanopatterning for secondary materials

Block copolymer thin films can be used as templates, either directly (as-coated) or indirectly (involving post-processing steps), to achieve secondary patterns of interest. Nanoparticle syntheses, nanolithography, and replication into elastomers are some of the areas where block copolymer surface nanopatterns have proved highly relevant as templates. These are discussed in the sections that follow.

Nanoparticle arrays

Arrays of nanoparticles on surfaces are interesting systems for electronics, optics, and sensing[54]. The creation of nanoparticle arrays using block copolymers as templates relies on chemical differences between the blocks in the block copolymer (Table 1).

Polymeric nanostructures are created either by making use of microphase-separated block copolymer thin films or block copolymer micelles preformed in solution and deposited onto surfaces as monolayers. One of the polymer blocks is chosen to fulfill a specific function, e.g. the binding of a precursor such as a metal ion. This leads to concentration of the precursors in one domain of the polymeric nanostructure. The nanoparticle arrays are then produced in a second treatment step, e.g. by a plasma treatment that destroys the polymer matrix and leaves behind metal or metal oxide particles. A special case is the use of organometallic block copolymers. Here, the metal that gives rise to a nanoparticle after plasma treatment is already present in the block copolymer. Organometallic block copolymers that contain Fe, Si, Zn, Sn, Pb, etc. have been synthesized[64-67].

GaAs nanostructures have been created by selective area growth on substrates patterned by polystyrene-*block*-polyisoprene (PS-*b*-PI) copolymers[68]. Kästle *et al.*[61] have shown a systematic change in dimensions of Au nanoparticles in the 1-15 nm range by using PS-P2VP reverse micelles as templates (Fig. 5). The tuning was achieved by loading the micelles to different extents by controlling the concentration of the precursor salt. Similar tunability has been shown by us and others[69]. In addition to *in situ* synthesis of nanoparticles, block-copolymer-derived templates can be used to assemble 'preformed' nanoparticles into a variety of ordered arrangements. The nanoparticle organization has been directed through selective chemical binding and purely physical means such as the use of capillary forces[70].

Nanoparticle arrays derived from block copolymers have been shown to be useful for biomolecule adhesion[63] and catalytic activity[71], and there are many other possibilities for benefiting from their optical, electronic, and magnetic properties.

Block copolymer lithography

Nanostructuring surfaces using block copolymers has relied on achieving a mass thickness contrast, i.e. patterning the polymer film

Table 1 Overview of the experimental approaches used to create nanoparticle arrays.

Template	Experimental means of including nanoparticles
Phase-separated block copolymer thin films	Vapor-phase deposition of reactive precursors into functional domains of the copolymer[55,56], e.g. formation of silicate nanostructures by tetraethoxysilane exposure of PS-*b*-PMMA films Electroless deposition[57,58]
Block copolymer micelles	Vapor-phase deposition[59], e.g. TiO_2 nanoparticles formed by depositing $TiCl_4$ precursors within the P2VP domains of PS-*b*-P2VP micelles on a surface Chemical reactions[60-63], e.g. Au nanoparticles by protonation of the PVP core of PS-*b*-P2VP micelles, Fe^{3+} included within carboxylic acid-containing polyacrylic acid (PAA) blocks of PS-*b*-PAA micelles

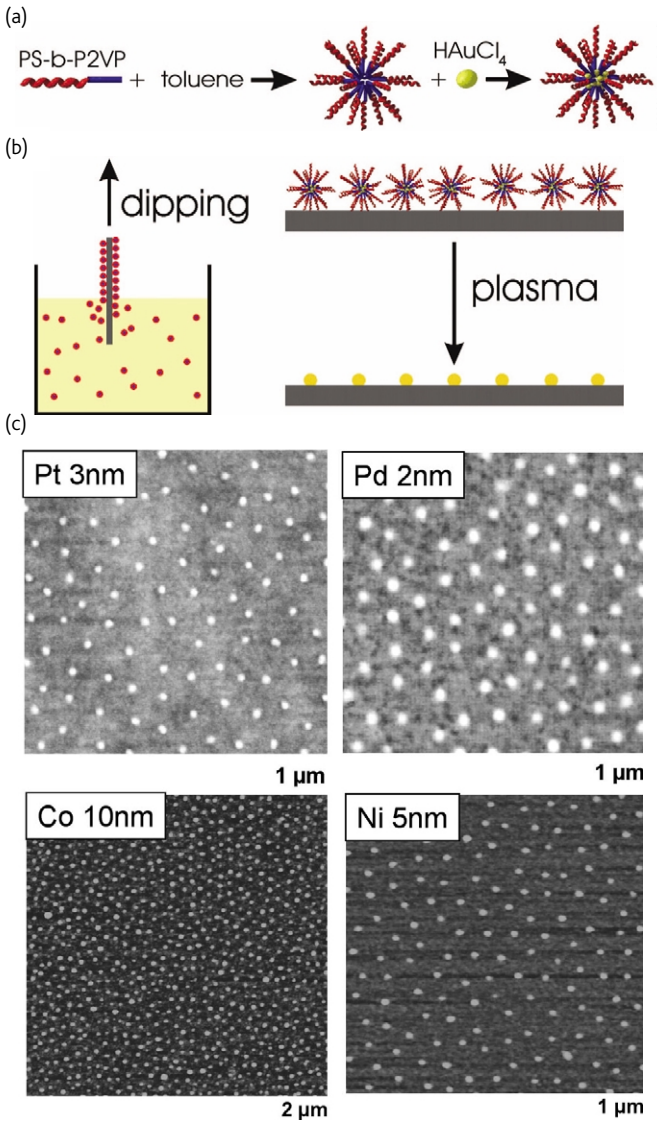

Fig. 5 (a, b) Schematic of the loading of micelles with metal salt in solution, followed by deposition on a surface by dip-coating. (c) AFM images of nanoparticles prepared from different elements using PS-P2VP micelles. (Adapted and reprinted with permission from[65]. © 2003 Wiley-VCH.)

thickness on the nanoscale, which is then transferred to the underlying substrate or replicated into another material. The primary means of achieving a mass thickness contrast in phase-separated block copolymer thin films is through selective degradation and removal of one of the domains (Table 2).

As well as structuring surfaces through a lithographic transfer by dry etching, it is possible to structure soft surfaces by the replication of the topographic contrast of the block copolymer patterns using elastomers such as poly(dimethylsiloxane) or PDMS. PDMS pillars and holes have been created by replicating an as-coated PS-P2VP micelle array[35] or a PS-PMMA porous template[82]. These surfaces are interesting to explore for use in bioimplants and bioactive bandages.

Applications of block copolymer surface nanopatterns

Photonic materials

The highly periodic lattices that can be achieved using block copolymer microphase separation in one, two, and three dimensions have attracted interest for the creation of photonic crystals[84]. Domains with dimensions on the order of optical wavelengths of interest need to be achieved, along with appropriate refractive index contrast and long-range domain orientation and order. Large domain dimensions are achievable using copolymers of high molecular weight, but this causes difficulties in handling because of high polymer viscosity. Other approaches have been proposed, such as swelling copolymer domains with a homopolymer. Urbas *et al.*[85,86] have used homopolystyrene to swell lamellar PS-PI microdomains to achieve repeat spacings appropriate for visible photonic applications. Fink *et al.*[87] have highlighted approaches for creating block-copolymer-based photonic crystals and the means of dealing with challenges in the system.

Enhancing the dielectric constant between the domains is necessary to achieve large photonic band gaps (PBGs). Preferential sequestering of optically transparent nanocrystals and selective chemical degradation of one of the blocks to create air pockets have been suggested as means of achieving high index contrast. Furthermore, the air channels can be backfilled with a high index material.

The use of block copolymers as PBG materials also offers attractive possibilities as a result of the functionality of the blocks, whose response to external stimuli can be read out as a change in reflectance for use in optical switches, couplers, and isolaters[88]. For instance, this could be used to detect chemo/bio-analytes with high sensitivity and selectivity[89]. The use of copolymers with liquid crystalline or elastomeric blocks has been proposed for achieving electrical or mechanical control over the reflectance spectrum, respectively[84,87].

Bioactive interfaces

Surface nanostructures have great potential in biological applications like diagnostic chips or implant surfaces that influence cell adhesion.

Sensing applications could benefit from the high surface-to-volume ratio of nanostructures and the possibility for selective chemical functionalization. The optical properties of nanoparticles such as Au and Ag offer further means of sensing binding events close to their surface through surface-enhanced spectroscopies[90]. Biofunctionalized Au particles created via nanosphere lithography have been used in localized surface plasmon resonance spectroscopy (LSPR)[91]. Spatz *et al.*[63] have shown biotin and streptavidin functionalization of an array of Au nanoparticles prepared using PS-P2VP micelles as templates.

There is growing interest in research on controlling cell adhesion and expression through surface topography[92-97]. Recently, Arnold *et al.*[98] used adhesive Au particle arrays with varying periodicities

Table 2 Overview of experimental approaches in block-copolymer lithography.

Template	Approach for achieving mass thickness contrast or etch contrast	Examples
Phase-separated block copolymer thin films	• Chemical etching and selective degradation of one of the blocks, e.g. ozone etching of PI domains in PS-*b*-PI copolymers, ultraviolet (UV) radiation degradation of PMMA in PS-*b*-PMMA copolymers[37,72-76]	• Holes in Si with different aspect ratios for microelectronics applications (Figs. 6 and 7)[72] • Polystyrene-block-polyferrocenyldimethylsilane (PS-*b*-PFS) to structure Si[67]
	• Chemical modification of one of the domains to enhance resistance, e.g. UV crosslinking of PI domains • Synthesis of block copolymers with an organometallic part, resulting in phase-separated organometallic domains that effectively resist plasma etching[26,67,77-80]	
Block copolymer micelles	• As-coated micellar thin films[81] • Binding of metal ions into micellar cores offering a higher resistance for etching[27]	• Si nanopatterned surface[81] • Polydimethylsiloxane (PDMS) pillars made by replicating hole-templates in PS-*b*-PMMA films[82] • GaAs pillars and holes[83]

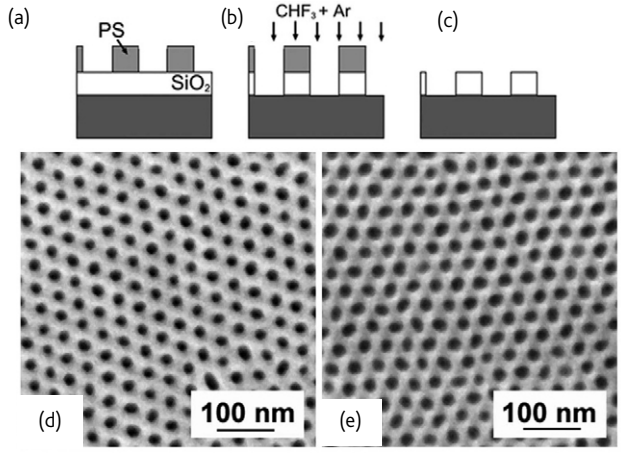

Fig. 6 Transfer of a self-assembled polymer template pattern into a dielectric film. The PS-PMMA block copolymer has a morphology of PMMA cylinders within a PS matrix. The PMMA block is degraded photochemically and the remaining PS forms the mask for the patterning of the SiO_2 sublayer. (a) Porous PS template formed on SiO_2. (b) Reactive ion etching (RIE) of the pattern into the oxide. (c) Strip PS mask. (d) SEM image of porous PS template on 20 nm thermal SiO_2. (e) SEM image of patterned oxide film on Si after removal of the PS mask (Adapted and reprinted with permission from[74]. © 2002 American Institute of Physics.)

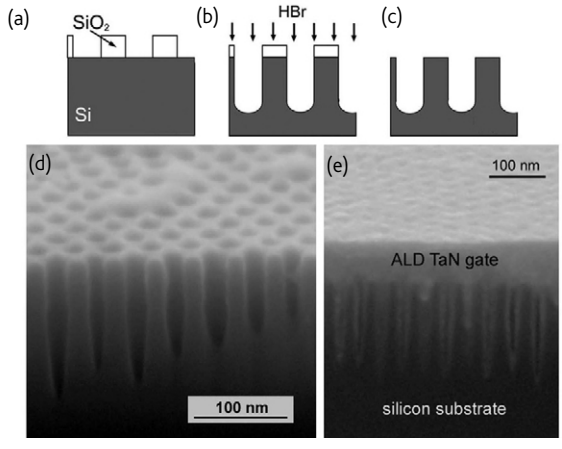

Fig. 7 High aspect ratio Si pore formation using a patterned oxide hard mask. Schematic of the process: (a) patterned SiO_2 on Si; (b) Si RIE using oxide hard mask; and (c) oxide removal. Tilted SEM images of (d) etched Si pores after oxide removal and (e) after atomic layer deposition of TaN to coat the oxidized trench sidewalls. Note that the apparent etch depth variations are artifacts of cleaving through the hexagonal array, which results in slices through different pore sections. (Adapted and reprinted with permission from[74]. © 2002 American Institute of Physics.)

prepared using PS-P2VP micelle arrays to identify the range of lengthscales for integrin clustering and activation. The choice of the right materials with nanopatterned surfaces and large-area processing capability are necessary to be able to realize useful technologies. Although it is now increasingly understood that the nanopatterns can influence cell behavior, the effects are different from case to case. This poses challenge for creating 'universal surfaces' capable of evoking a common response or designing surfaces that can evoke a desired response from a target cell.

Summary

The self-assembly of block copolymer systems is a promising way to create structures on the nanometer scale. As we gain a deeper understanding of the underlying processes, we will achieve better control of feature size and properties. The simplicity of this very versatile toolbox-like approach, along with its potential low cost for generating small features over large areas, makes it very interesting for applications in various different fields. First examples are shown here, and many more applications are likely to appear in the future. mt

Acknowledgments

The generous support of the Office Fédéral de l'Education et de la Science (OFES) and the National Competence Center for Research (NCCR) in Nanoscale Science in Switzerland, as well as the European research and training networks POLYNANO and BioPolysurf, are gratefully acknowledged.

REFERENCES

1. Hamley, I. W., *Angew. Chem. Int. Ed.* (2003) **42**, 1692
2. Li, H., and Huck, W. T. S., *Curr. Opin. Solid State Mater. Sci.* (2002) **6**, 3
3. Liu, T., *et al., Prog. Polym. Sci.* (2003) **28**, 5
4. Bates, F. S., and Fredrickson, G. H., *Phys. Today* (1999) **52**, 32
5. Hamley, I. W., *Nanotechnology* (2003) **14**, R39
6. Ikkala, O., and ten Brinke, G., *Chem. Commun.* (2004) 2131
7. Mansky, P., *et al., Macromolecules* (1997) **30**, 6810
8. Huang, E., *et al., Macromolecules* (1998) **31**, 7641
9. Heier, J., *et al., Macromolecules* (1997) **30**, 6610
10. Heier, J., *et al., J. Chem. Phys.* (1999) **111**, 11101
11. Peters, R. D., *et al., Langmuir* (2000) **16**, 9620
12. Carvalho, B. L., and Thomas, E. L., *Phys. Rev. Lett.* (1994) **73**, 3321
13. Kellogg, G. J., *et al., Phys. Rev. Lett.* (1996) **76**, 2503
14. Russell, T. P., *et al., Macromolecules* (1991) **24**, 6263
15. Turner, M. S., and Joanny, J. F., *Macromolecules* (1992) **25**, 6681
16. Walton, D. G., *et al., Macromolecules* (1994) **27**, 6225
17. Spatz, J. P., *et al., Macromolecules* (2000) **33**, 150
18. Fasolka, M. J., *et al., Phys. Rev. Lett.* (1997) **79**, 3018
19. Knoll, A., *et al., Phys. Rev. Lett.* (2002) **89**, 035501
20. Rehse, N., *et al., Macromolecules* (2003) **36**, 3261
21. Rockford, L., *et al., Phys. Rev. Lett.* (1999) **82**, 2602
22. Yang, X. M., *et al., Macromolecules* (2000) **33**, 9575
23. Segalman, R. A., *et al., Adv. Mater.* (2001) **13**, 1152
24. Kim, S. O., *et al., Nature* (2003) **424**, 411
25. Xiao, S., *et al., Nanotechnology* (2005) **16**, S324
26. Cheng, J. Y., *et al., Appl. Phys. Lett.* (2002) **81**, 3657
27. Glass, R., *et al., Nanotechnology* (2003) **14**, 1153
28. Glass, R., *et al., New J. Phys.* (2004) **6**, 101
29. Meister, A., *et al., Microelectron. Eng.* (2006), in press
30. Möller, M., *et al., Adv. Mater.* (1996) **8**, 337
31. Krishnamoorthy, S., *et al., Langmuir* (2006) **22**, 3450
32. Fu, J., *et al., Macromolecules* (2004) **37**, 976
33. Choucair, A., and Eisenberg, A., *Eur. Phys. J. E* (2003) **10**, 37
34. Meiners, J. C., *et al., Appl. Phys. A* (1995) **61**, 519
35. Krishnamoorthy, S., *et al., Adv. Func. Mater.* (2006) **16**, 1469
36. Xu, T., *et al., Polymer* (2001) **42**, 9091
37. Guarini, K. W., *et al., Adv. Mater.* (2002) **14**, 1290
38. Thurn-Albrecht, T., *et al., Science* (2000) **290**, 2126
39. Bal, M., *et al., Appl. Phys. Lett.* (2002) **81**, 3479
40. Kim, H.-C., *et al., Adv. Mater.* (2001) **13**, 795
41. Yang, X., *et al., J. Vac. Sci. Technol. B* (2004) **22**, 3331
42. Peng, J., *et al., J. Chem. Phys.* (2005) **122**, 114706
43. Mayes, A. M., *et al., Macromolecules* (1992) **25**, 6523
44. Winey, K. I., *et al., Macromolecules* (1991) **24**, 6182
45. Tanaka, H., *et al., Macromolecules* (1991) **24**, 240
46. Hashimoto, T., *et al., Macromolecules* (1990) **23**, 4378
47. La, Y.-H., *et al., Nano Lett.* (2005) **5**, 1379
48. Sidorenko, A., *et al., J. Am. Chem. Soc.* (2003) **125**, 12211
49. Xu, T., *et al., Macromolecules* (2004) **37**, 2972
50. Xu, T., *et al., Adv. Func. Mater.* (2003) **13**, 698
51. Sohn, B.-H., *et al., J. Am. Chem. Soc.* (2001) **123**, 12734
52. Elbs, H., *et al., Macromolecules* (1999) **32**, 1204
53. Brittain, W. J., *et al., Abstr. Papers Am. Chem. Soc.* (2004) **227**, U472
54. Shipway, A. N., *et al., ChemPhysChem* (2000) **1**, 18
55. Melde, B. J., *et al., Chem. Mater.* (2005) **17**, 4743
56. Abes, J. I., *et al., Chem. Mater.* (2003) **15**, 1125
57. Wang, T. C., *et al., Chem. Mater.* (2003) **15**, 299
58. Boontongkong, Y., *et al., Chem. Mater.* (2000) **12**, 1628
59. Li, X., *et al., Langmuir* (2005) **21**, 5212
60. Boontongkong Y., and Cohen, R. E., *Macromolecules* (2002) **35**, 3647
61. Kästle, G., *et al., Adv. Func. Mater.* (2003) **13**, 853
62. Boyen, H.-G., *et al., Adv. Func. Mater.* (2003) **13**, 359
63. Spatz, J. P., *et al., Langmuir* (2000) **16**, 407
64. Sankaran, V., *et al., Chem. Mater.* (1993) **5**, 1133
65. Chan, Y. N. C., *et al., Chem. Mater.* (1992) **4**, 885
66. Cummins, C. C., *et al., Chem. Mater.* (1991) **3**, 1153
67. Lammertink, R. G. H., *et al., Chem. Mater.* (2001) **13**, 429
68. Li, R. R., *et al., Appl. Phys. Lett.* (2000) **76**, 1689
69. Aizawa, M., and Buriak, J. M., *J. Am. Chem. Soc.* (2005) **127**, 8932
70. Misner, M. J., *et al., Adv. Mater.* (2003) **15**, 221
71. Hinderling, C., *et al., Adv. Mater.* (2004) **16**, 876
72. Black, C. T., *et al., IEEE Electron Device Lett.* (2004) **25**, 622
73. Guarini, K. W., *et al., J. Vac. Sci. Technol. B* (2002) **20**, 2788
74. Guarini, K. W., *et al., J. Vac. Sci. Technol. B* (2001) **19**, 2784
75. Black, C. T., *et al., Appl. Phys. Lett.* (2001) **79**, 409
76. Park, M., *et al., Science* (1997) **276**, 1401
77. Cheng, J. Y., *et al., IEEE Trans. Magn.* (2002) **38**, 2541
78. Cheng, J. Y., *et al., Adv. Mater.* (2001) **13**, 1174
79. Lammertink, R. G. H., *et al., J. Polym. Sci., Part B: Polym. Phys.* (1999) **37**, 1009
80. Cheng, J. Y., *et al., Phys. Rev. B* (2004) **70**, 064417
81. Meli, M.-V., *et al., Nano Lett.* (2002) **2**, 131
82. Kim, D. H., *et al., Adv. Mater.* (2003) **15**, 811
83. Spatz, J. P., *et al., Adv. Mater.* (1999) **11**, 149
84. Edrington, A. C., *et al., Adv. Mater.* (2001) **13**, 421
85. Urbas, A., *et al., Macromolecules* (1999) **32**, 4748
86. Urbas, A., *et al., Adv. Mater.* (2000) **12**, 812
87. Fink, Y., *et al., J. Lightwave Technol.* (1999) **17**, 1963
88. Mao, G., *et al., Chem. Mater.* (1998) **10**, 1538
89. Alivisatos, P., *Nat. Biotechnol.* (2004) **22**, 47
90. Chumanov, G., *et al., J. Phys. Chem.* (1995) **99**, 9466
91. Riboh, J. C., *et al., J. Phys. Chem. B* (2003) **107**, 1772
92. Niemeyer, C., and Mirkin, C., (eds.), *Nanobiotechnology*, Wiley-VCH Verlag, Weinheim, Germany, (2004), 53
93. Curtis, A. S. G., and Wilkinson, C. D., *J. Biomater. Sci.: Polym. Ed.* (1998) **9**, 1313
94. Dalby, M. J., *et al., Biomaterials* (2002) **23**, 2945
95. Wilkinson, C. D. W., *et al., Mater. Sci. Eng. C* (2002) **19**, 263
96. Dalby, M. J., *et al., J. Biomed. Mater. Res., Part A* (2003) **67A**, 1025
97. Krishnamoorthy, S., *et al.*, (2006) unpublished results
98. Arnold, M., *et al., ChemPhysChem* (2004) **5**, 383